Rotation Effects on Streamline Topology and their Bifurcation of Stagnation Points Analysis for Peristaltic Flows of Bingham Fluid

المؤتمر العربي الدولي الأول في الرياضيات الصناعية والطبية في بريطانيا

The First Arab International Conference In Industriel And Medical Mathematics In Britain

من تنظيم اكاديمية القاموس للأبحاث والترجمة بالتنسيق مع شبكة الجالية الجزائرية

Conference Organized By: Qamous Academy For Research And Translation In Collaboration With Algerian Diaspora Network

A General Systems Theory Of Marriage: Nonlinear Difference Equation Modeling Of Marital Interaction

م.م زين العابدين الصافي / جامعة واسط

Abstract

In this work, we focus the impact of rotation on the streamline patterns and their local and global bifurcation on the symmetric peristaltic flow of non-Newtonian fluid in 2_dimensional coordinates. The analytical solution depending the conditions to find the stream function under incompressible Bingham fluid, long-wavelength and small Reynolds number. This problem is solution in a move the planer system when the system nonlinear autonomous differential equations. There are three cases of flow appear themselves, backward, trapping and augment flow, will be discussing in this research. We have discussed different values of rotation, wave rate and amplitude ratio and effects on the bifurcation and their topological changes graphically through the set of figures. All these bifurcations are summarized through global bifurcation diagram. Numerical results have been computed by using MATHEMATICA software via perturbation method.

Keywords: peristaltic flow, bifurcation, stability, rotation, velocity, stream function , stress, viscoplastic.

1- Introduction

Topological fluid dynamics is a mathematical specialty that studies topological countenance of flows with complex trajectories and their implementations to motions fluid, and evolve group theoretic and geometric points of opinion on many problems of hydrodynamical origin. It is located at intersection of different specialty, including Lie group, stability theory, partial differential equations, knot theory , integrable systems and geometric inequalities. The peristaltic pumping is known with special type pumping when it can easily be transported the variety of complex rheological fluids from one place to another place. This pumping precept is called peristaltic. This mechanism responsible for the flow of blood in arterioles, transport of urine from the kidney to the bladder through the ureter and passage of lymph through lymphatic vessels. Applications of peristaltic in industrial fluid mechanics are like aggressive chemical, high solid slurries, noxious (nuclear industries) and several experimental and theoretical studies the peristaltic transport in both the physiological and mechanical situation under various approximation. The vast applications of peristalsis has been attracting the interests of researchers after the seminal work of Latham[1]. Jaffrin, M.Y., Shapiro [2] investigated peristaltic transport in a move frame for Newtonian fluid under long-wavelength.

Abd-Alla and Abo-Dahab [3,4] Investigate the effect the rotation and initial stress on the peristaltic flow of an incompressible. In physiology, peristalsis is used to transport the biofluid from a region of lower pressure to higher pressure in the living body [5]. Peristaltic pumps have become popular to pump and/or dose complex fluids, due to their robustness [6]. Analyze the behavior of second-grade dusty fluid flowing through a flexible tube whose walls are induced by the peristaltic movement [7]. The peristaltic transport of power-law fluid in an elastic tapered tube with variable cross-section induced by dilating peristaltic wave [8] peristaltic transport of a Herschel–Bulkley fluid in an axisymmetric tube. The governing equations are solved using the long wavelength and small Reynolds number approximation [9].

What was done mentioned earlier is clarify the trapping phenomenon cases, but not did touch on or discussed or using method dynamical system with respect of the bifurcations and stability of equilibrium points. In peristaltic transport the bifurcation exist when small change in interested of parameters causes a surprising topological change in its flow demeanor. Some may have preceded us in studying, Joel Jiménez-Lozano and Mihir Sen [10] studied the streamline topologies of two-dimensional peristaltic flow and their bifurcations for the symmetric channel. Asghar and Ali [11,12] extended the study of Joel Jiménez-Lozano and Mihir Sen by explaining convective and slip effects. Ali and Ullah [13,15] investigated the bifurcation analysis for peristaltic transport of a power-law fluid. Ullah et al. [14] explained the bifurcation and stability analysis of critical/stagnation points for peristaltic transport of a power-law fluid in a tube. Ullah, and Ali [16] expanded to A study on bifurcation of stagnation points for a peristaltic transport of micropolar fluids with slip condition. Ullah et al. [14] explained the bifurcation and stability analysis of critical/stagnation points for peristaltic transport of a power-law fluid in a tube. M. A. Murad [17] applied the bifurcation and stability for Bingham fluid.

In this paper, we will study the rotation effects on the bifurcation and stability of the equilibrium points by giving different values of rotation, amplitude ratio, rate of flow. Applied this work on the Bingham fluid with the axisymmetric peristaltic flow with dynamic system. Display changes in bifurcation through many graphs.

2- Formulation of the problem

Let us the peristaltic flow of an incomperssiable Bingham fluid in an axisymmetric channel of width (2α) in a two-dimensional cartesian coordinates with flexible walls and. The flow is generated by continously moving sinusoidal wave trains on channel walls with speed c. The channel walls are show in figure (1) and d

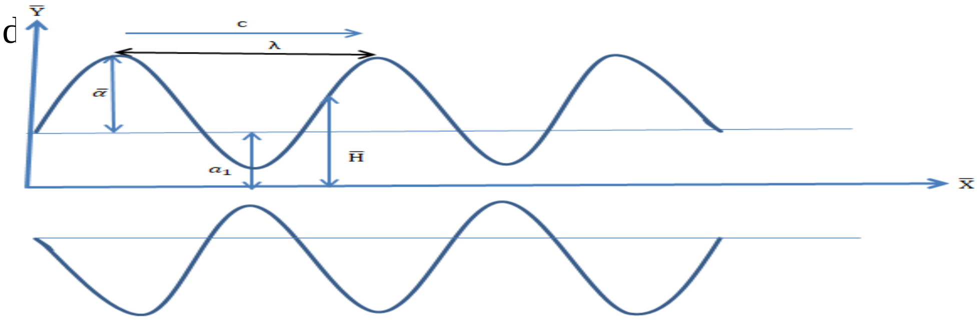

Figure 1. Schematic Diagram

$$\bar{H}(\bar{X},\bar{t}) = a_1 - \bar{\alpha}\left(1 - \mathrm{Sin}^2\left(\frac{\pi}{\lambda}(\bar{X} - c\bar{t})\right)\right) \tag{1}$$

Where a_1 is total wave heigh, $\bar{\alpha}$ the amplitude wave, λ the wavelength and $\bar{t}$ is the time. The governed equations of the flow by two coupled nonlinear partial differential of continuity and momentum which in frame $(\bar{X}\,,\bar{Y})$ are expressed as:

$$\frac{\partial \bar{U}}{\partial \bar{X}} + \frac{\partial \bar{V}}{\partial \bar{Y}} = 0, \tag{2}$$

$$\rho\left(\frac{\partial}{\partial \bar{t}} + \bar{U}\frac{\partial}{\partial \bar{X}} + \bar{V}\frac{\partial}{\partial \bar{Y}}\right)\bar{U} - \rho\Omega\left(\Omega\bar{U} + 2\,\frac{\partial \bar{V}}{\partial \bar{t}}\right) = -\frac{\partial \bar{P}}{\partial \bar{X}} + \frac{\partial \bar{S}_{\bar{X}\bar{X}}}{\partial \bar{X}} + \frac{\partial \bar{S}_{\bar{X}\bar{Y}}}{\partial \bar{Y}} \tag{3}$$

$$\rho\left(\frac{\partial}{\partial \bar{t}} + \bar{U}\frac{\partial}{\partial \bar{X}} + \bar{V}\frac{\partial}{\partial \bar{Y}}\right)\bar{V} - \rho\Omega\left(\Omega\bar{V} - 2\,\frac{\partial \bar{U}}{\partial \bar{t}}\right) = -\frac{\partial \bar{P}}{\partial \bar{X}} + \frac{\partial \bar{S}_{\bar{Y}\bar{X}}}{\partial \bar{X}} + \frac{\partial \bar{S}_{\bar{Y}\bar{Y}}}{\partial \bar{Y}} \tag{4}$$

Where ρ is fluid density, $\bar{\mathbf{V}} = [\bar{U},\bar{V}]$ velocity components, $\bar{P}$ is pressure, $\bar{S}_{\bar{X}\bar{X}}$, $\bar{S}_{\bar{X}\bar{Y}}$ and $\bar{S}_{\bar{Y}\bar{Y}}$ are the compenent of extra stress tensor $\bar{S}$, Ω is the rotation, $\nabla = [\frac{\partial}{\partial \bar{X}}, \frac{\partial}{\partial \bar{Y}}]$, σ is the cauchy stress tensor which for the Bingham plastic fluid is defined [19]:

$$\sigma = -\bar{P}\,\bar{I} + \bar{S} \tag{5}$$

where,

$$\bar{S} = 2\mu\omega + 2\tau_0\,\hat{\omega} \tag{6}$$

In equation (6) $\tau_0$is the yield stress while the rate of deformation tensor ω and $\hat{\omega}$ is the tensor are defined:

$$\omega=\frac{1}{2}\ (\nabla\bar{V}+\ (\nabla\bar{V})^T)\ )\ ,\quad \widehat{\omega}\ =\frac{\omega}{\sqrt{2\ tra\ \omega^2}} \tag{7}$$

in view of equation (6,7) the compenents of extra stress tensor in laboratory frame become

$$\bar{S}_{\bar{X}\bar{X}} = 2\ \mu\ \omega_{\bar{X}\bar{X}} + \frac{2\tau_0\omega_{\bar{X}\bar{X}}}{\sqrt{2tr\omega^2}}\ ,\ \bar{S}_{\bar{X}\bar{Y}} = 2\ \mu\ \omega_{\bar{X}\bar{Y}} + \frac{2\tau_0\omega_{\bar{X}\bar{Y}}}{\sqrt{2tr\omega^2}},\ \bar{S}_{\bar{Y}\bar{Y}} = 2\ \mu\ \omega_{\bar{Y}\bar{Y}} + \frac{2\tau_0\omega_{\bar{Y}\bar{Y}}}{\sqrt{2tr\omega^2}} \tag{8}$$

Peristaltic motion in natural unsteady phenomenon but it can be assumed steady by using the transformation from laboratory fram(fixed frame) $(\bar{X},\bar{Y})$ to wave frame(move frame) $(\bar{x},\bar{y})$. The relationship between coordinates, velocities and pressure in laboratory fram $(\bar{X},\bar{Y})$ and wave frame $(\bar{x},\bar{y})$ is provided by the following transformations

$$\bar{x} = \bar{X} + \mathrm{c}\bar{t},\ \ \bar{y} = \bar{Y},\ \ \bar{u} = \bar{U} - \mathrm{c},\ \ \bar{v} = \bar{V},\ \ \bar{p}(\bar{x},\bar{y}) = \bar{P}(\bar{X},\bar{Y},\bar{t}) \tag{9}$$

Where $\bar{u},\bar{v}, and\ \bar{p}$ are velocity compenents and pressure in wave frame. Now, we transform equations (1,2,3,4,8) in wave frame with help of equation (9) and normalize the resulting equation by using following dimensionless quantities:

$$\bar{x} = \frac{\lambda x}{\pi},\ \ \bar{y} = a_1 y,\ \ \bar{u} = cu\ ,\ \bar{v}=\delta cv,\ \bar{t} = \frac{\lambda}{c\pi}\ t,\ \bar{p} = \frac{c\mu}{\pi {a_1}^2}\lambda \mathrm{p},\ R_e = \frac{\rho a_1 c}{\mu},\ \bar{\alpha} = \emptyset a_1,\ \ \ \delta = \frac{\pi a_1}{\lambda},$$
$$\bar{H}=ha_1,\ \ \bar{S}=\frac{c\mu}{a_1}\ S,\ \ \ B_n = \frac{a_1\tau_0}{\mu c}.$$

To obtain,

$$h(x) = 1 - \emptyset(1 - \ Sin^2(x)) \tag{10}$$

where $0 < \emptyset < 1$, is the amplitude ratio. Also the equations (2,3,4,8) in dimensionless frams is:

$$\delta\frac{\partial u}{\partial x} + \ \frac{\partial v}{\partial y} = 0 \tag{11}$$

$$R_e\delta\left(u\frac{\partial u}{\partial x} + v\frac{\partial u}{\partial y}\right) - \frac{\rho {a_1}^2}{\mu}\Omega^2 u = -\ \frac{\partial p}{\partial x} + \ \delta\frac{S_{xx}}{\partial x} + \ \frac{\partial S_{xy}}{\partial y} \tag{12}$$

$$R_e\delta^2\left(u\frac{\partial v}{\partial x} + v\frac{\partial v}{\partial y}\right) - \delta\frac{\rho\Omega^2 {a_1}^2 v}{\mu} - 2\Omega\ R_e\delta^2 u\frac{\partial u}{\partial t} = -\ \frac{\partial p}{\partial y} + \delta^2\frac{\partial S_{yx}}{\partial x} + \delta\frac{\partial S_{yy}}{\partial y} \tag{13}$$

$$S_{xx} = 2\delta\frac{\partial u}{\partial x} + \frac{2\delta B_n(\frac{\partial u}{\partial x})}{\sqrt{2\delta^2(\frac{\partial u}{\partial x})^2 + 2(\frac{\partial v}{\partial y})^2 + \ (\frac{\partial u}{\partial y} + \delta\frac{\partial v}{\partial x})^2}} \tag{14}$$

$$S_{xy} = S_{yx} = \left(\frac{\partial u}{\partial y} + \delta^2\frac{\partial v}{\partial x}\right) + B_n\frac{\left(\frac{\partial u}{\partial y} + \delta^2\frac{\partial v}{\partial x}\right)}{\sqrt{2\delta^2\ (\frac{\partial u}{\partial x})^2 + 2\ (\frac{\partial v}{\partial y})^2 + (\frac{\partial u}{\partial y} + \ \delta\frac{\partial v}{\partial x})^2}} \tag{15}$$

$$S_{yy} = 2\delta\frac{\boldsymbol{\partial v}}{\boldsymbol{\partial y}} + \ \frac{2\delta B_n(\frac{\partial v}{\partial y})}{\sqrt{2\delta^2(\frac{\partial u}{\partial x})^2 + 2(\frac{\partial v}{\partial y})^2 + \ (\frac{\partial u}{\partial y} + \delta\frac{\partial v}{\partial x})^2}} \tag{16}$$

In above equations, the dimensionless number, δ is the wave number, B_n is Bingham number, R_e Reynolds number. Introduction to the stream function (ψ) by relation:

$u = \psi_y, \;\; v = -\delta\psi_x.$

From equations(11-16) show that the continuity equation (11) satisfies identically while other equations take the following form:

$$R_e\delta\left(\psi_y\frac{\partial\psi_y}{\partial x} - \psi_x\frac{\partial\psi_y}{\partial y}\right) - \frac{\Omega^2{a_1}^2\rho}{\mu}\psi_y + 2R_e\delta^2\frac{\partial\psi_x}{\partial t} = -\frac{\partial p}{\partial x} + \delta\frac{\partial S_{xx}}{\partial x} + \frac{\partial S_{xy}}{\partial y} \qquad (17)$$

$$-R_e\delta^3\left(\psi_y\frac{\partial\psi_x}{\partial x} - \delta\,\psi_x\frac{\partial\psi_x}{\partial y}\right) - \frac{\Omega^2{a_1}^2\rho}{\mu}\delta^2\,\psi_x + 2\Omega R_e\delta^2\psi_y\frac{\partial\psi_y}{\partial t} = -\frac{\partial p}{\partial y} + \delta\frac{\partial S_{xx}}{\partial y} + \delta^2\frac{\partial S_{xy}}{\partial x} \qquad (18)$$

$$S_{xx} = 2\delta\psi_{xy} + \frac{2\delta B_n\psi_{xy}}{\sqrt{2\delta^2(\psi_{xy})^2 + 2\delta^2(\psi_{xy})^2 + (\psi_{yy} - \delta^2\psi_{xx})^2}} \qquad (19)$$

$$S_{xy} = S_{yx} = (\psi_{yy} - \delta^3\psi_{xx}) + \frac{B_n(\psi_{yy} - \delta^3\psi_{xx})}{\sqrt{2\delta^2(\psi_{xy})^2 + 2\delta^2(\psi_{xy})^2 + (\psi_{yy} - \delta^2\psi_{xx})^2}} \qquad (20)$$

$$S_{yy} = -2\delta\psi_{xy} - \frac{2\delta B_n\psi_{xy}}{\sqrt{2\delta^2(\psi_{xy})^2 + 2\delta^2(\psi_{xy})^2 + (\psi_{yy} - \delta^2\psi_{xx})^2}} \qquad (21)$$

The equations from(17-21) when ($R_e\ and\ \delta \ll 1$) are become in the form:

$$-\frac{\Omega^2{c_1}^2\rho}{\mu}\psi_y = -\frac{\partial p}{\partial x} + \frac{\partial S_{xy}}{\partial y} \qquad (22)$$

$$-\frac{\partial p}{\partial y}=0 \qquad (23)$$

Whereas the component of extra stess tensor become in the form:

$$S_{xy} = \psi_{yy} + B_n\,,\; S_{yy} = 0, \qquad S_{xx} = 0. \qquad (24)$$

substituting equation (24) into (22) and derivting with respect of y, we get high nonlinear differential equations:

$$\frac{\partial^2}{\partial y^2}(\psi_{yy} + B_n) + \frac{\Omega^2{a_1}^2\rho}{\mu}\psi_{yy}=0 \qquad (25)$$

And the final equation become to:

$$\psi_{yyyy} + \frac{\Omega^2{a_1}^2\rho}{\mu}\psi_{yy}=0 \qquad (26)$$

the dimensionless volume flow rate and boundary condition in the wave frams are [10,11]:

$$\psi = 0, \quad \psi_{yy} = 0, \quad at\ y = 0 \tag{27}$$

$$\psi = q, \quad \psi_y = -1, \quad at\ y = h \tag{28}$$

$$q\text{-}1 = F = \int_0^h \frac{\partial \psi}{\partial y} dy = \psi(h) - \psi(0) \tag{29}$$

q and F are the dimensionless mean flow rate in fixed and wave frams respectively.

3- Solution of the Problem

The solution of equation (26) subject to boundary condition (27,28) is

$$\psi = \frac{\sqrt{k} q y \mathrm{Cos}[h\sqrt{k}] + y \mathrm{Sin}[h\sqrt{k}] - (h+q)\mathrm{Sin}[\sqrt{k} y]}{h\sqrt{k}\mathrm{Cos}[h\sqrt{k}] - \mathrm{Sin}[h\sqrt{k}]} \tag{30}$$

Where k= $\frac{\Omega^2 {a_1}^2 \rho}{\mu}$.

Three different flow situation occure, namely, augmented, trap and backward flow. Where the streamline splits to enclose an amount of fluid called a bolus, this situation is trapping, when the trapped bolus splits and exist some flows going in the forward direction is said to be augmented and when the flow goes in direction opposite to the traveling wave is said backward flow. On anslyzing solution (30) clearly the three situation of the flow in figure (2).

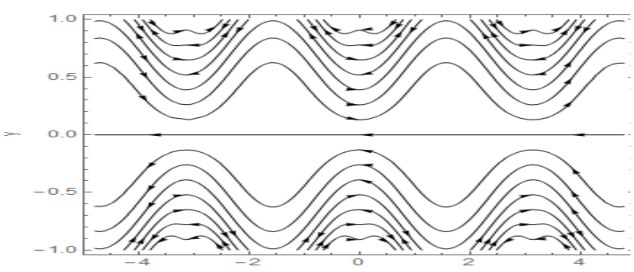

(i) Backward flow: q= -2/5, $\Omega = 2.0, \phi = 0.6$

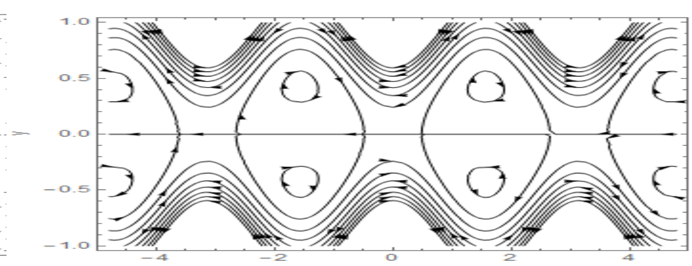

(ii) Trapping: q= -0.18, $\Omega = 2.0, \phi = 0.6$

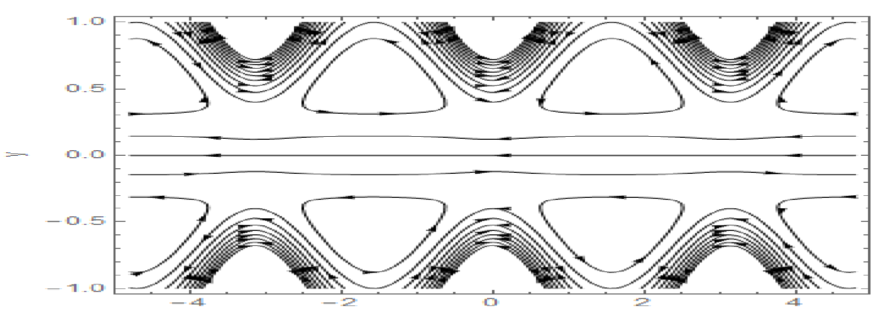

(iii) augmented flow: $q = 1/10, \Omega = 2.0, \phi = 0.6$

Figure 2. Streamlines patterns of various flow situation in the wave frame of reference.

4- Nonlinear dynamical system for flow field

In this section we apply the ideas from qualitative theory of dynamical system which employs to detect the behavior, stability and bifurcation of equilibrium in the flow. The present proplem can obtain the axial and transverse velocity components by reduce to as a system of nonlinear autonomous system by using the relation u=$\frac{\partial\psi}{\partial y}$ and v= - $\frac{\partial\psi}{\partial x}$. Equation (30) become to:

$$\frac{\sqrt{k}(q\text{Cos}[h\sqrt{k}]-(h+q)\text{Cos}[\sqrt{k}y])+\text{Sin}[h\sqrt{k}]}{h\sqrt{k}\text{Cos}[h\sqrt{k}]-\text{Sin}[h\sqrt{k}]}=\text{f(x,y,ß)} \tag{31}$$

$$\frac{\sqrt{k}(2\sqrt{k}(-1+\text{Cos}[\sqrt{k}y]\text{Cos}[\sqrt{k}h])h+2\text{Cos}[\sqrt{k}y](-1+kh(q+h))\text{Sin}[\sqrt{k}h]-2\sqrt{k}q\text{Sin}[\sqrt{k}h]^2+\text{Sin}[2\sqrt{k}h])\text{h1}}{2(-\sqrt{k}\text{Cos}[\sqrt{k}h]h+\text{Sin}[\sqrt{k}h])^2}=\text{g(x,y,ß)} \tag{32}$$

Where ß=(q, Ø,k), $-\infty < x < \infty$ and $-h < y < h$ are the domain interest. The value of amplitude ratio ranges $0 < \emptyset < 1$ and $h1 = \frac{\partial h}{\partial x}$. Sitting f(x,y,ß)= g(x,y,ß)=0 in the flow field to obtain the critical points [20] and apply the Hurtman Grobman theorem, by using Jacobian to found the critical point according to which the nature of this critical point. If the critical point is degnerate if the determinant of Jacobian at a certain critical point is zero. There are two subcategories degeneracies (simple, non-simple). When the eigenvalues of the Jacobian are zero is called simple degeneracy whereas if the Jacobian is a zero matrix is called non-simple degeneracy. Using Bakker notation [21] to classification of the critical points in two dimension system. The classification of the phase given in terms of trace: $\tau = \lambda_1 + \lambda_2$ and the Jacobian : $\zeta = \lambda_1 * \lambda_2$, where $\lambda_1\, and\, \lambda_2$ are eigenvalues. According [22] a bifurcation point with respect to parameter ß is a solution of (x,y, ß) at which the number of equilibrium, periodic or quasi-priodic solutions changes when ß passes through ß$_c$, with ß$_c$ as critical value. The critical points are given by:

1. $\{x_{1,2}, y_{1,2}\}$ = {nπ, $\pm\frac{\sqrt{-2\sqrt{k}(-1-q+\phi+q\text{Cos}[\sqrt{k}(-1+\phi)])+2\text{Sin}[\sqrt{k}(-1+\phi)]}}{\sqrt{k^{3/2}(1+q-\phi)}}$ }, n∈ Z

2. $\{x_{3,4}, y_{3,4}\}$ = {$\pm\frac{\sqrt{A+2*B\text{Cos}[B]-\sqrt{k}q\text{Cos}[2*B]+(2*C*D)\text{Sin}[B]+\text{Sin}[2*B]}}{\sqrt{2}\sqrt{\sqrt{k}\phi(E*\text{Cos}[B]+\text{Cos}[2*B]+\sqrt{k}(F+2q\text{Cos}[B])\text{Sin}[B])}}$, 0},

3. $\{x_{5,6}, y_{5,6}\}$ = {(2n-1)π/2 , $\pm\frac{\sqrt{2\sqrt{k}(1+q-q\text{Cos}[\sqrt{k}])-2\text{Sin}[\sqrt{k}]}}{\sqrt{k^{3/2}(1+q)}}$ }, n∈ Z, where

$A = \sqrt{k}(2+q-2\phi), B = \sqrt{k}(-1+\phi), C = -1-k(1+q-\phi), D = -1+\phi, E = -1+k(-1+\phi)(-1-q+\phi)\; and\; F = -1-q+\phi$. In next section we will classification of the critical points are present as will as the local and global bifurcation diagrams for this points.

4.1- the stegnation points $\{x_{1,2}, y_{1,2}\}$

The critical points $\{x_{1,2}, y_{1,2}\}$, are cropped up under the wave crest. The Jacobian matrix is

$$J|_{\{x_{1,2}\,,\,y_{1,2}\}}=\begin{bmatrix} 0 & ss_1 \\ ss_2 & 0 \end{bmatrix}$$

$$ss_1=\pm\frac{k\,B1\,\mathrm{Sin}[\frac{\sqrt{k}\sqrt{-2\sqrt{k}(B1+q\mathrm{Cos}[\mathrm{A1}])+2\mathrm{Sin}[\mathrm{A1}]}}{\sqrt{-k^{3/2}\,B1}}]}{\sqrt{k}(-1+\phi)\mathrm{Cos}[\sqrt{k}(-1+\phi)]+\mathrm{Sin}[\sqrt{k}(1-\phi)]},$$

$$ss_2=$$

$$\pm(\sqrt{k}\phi(2\mathrm{A1}+2\mathrm{Cos}[\frac{\sqrt{-2\sqrt{k}(B1+q\mathrm{Cos}[\mathrm{A1}])+2\mathrm{Sin}[\mathrm{A1}]}}{k^{1/4}\sqrt{1+q-\phi}}](-\mathrm{A1}\,\mathrm{Cos}[\mathrm{A1}]+C1D1\mathrm{Sin}[\mathrm{A1}])-2\sqrt{k}q\mathrm{Sin}[\mathrm{A1}]^2-\mathrm{Sin}[2\mathrm{A1}])))\Big/\mathrm{E1}$$

Where

$\mathrm{A1}=\sqrt{k}(-1+\phi);\mathrm{B1}=(-1-q+\phi);\mathrm{C1}=-1-k(1+q-\phi);\mathrm{D1}=-1+\phi,E1=(\mathrm{A1Cos}[\mathrm{A1}]+\mathrm{Sin}[\mathrm{A1}])])^2.$

The eigenvalues are

$$\lambda_{1,2} = \pm((\sqrt{k}\surd(-\sqrt{k}\phi(B1)(A1)Cos[A1])]-Sin[A1])(\sqrt{k}(2+q-2\phi)-\sqrt{k}qCos[2\,A1]+ 2Cos[\frac{\sqrt{-2\sqrt{k}(B1+qCos[A1])+2Sin[A1]}}{k^{1/4}\sqrt{-B1}}](A1\,Cos[A1]\;+C1\,D1\,Sin[A1])+Sin[2A1])Sin[\frac{\sqrt{k}\sqrt{-2\sqrt{k}(B1+qCos[A1])+2Sin[A1]}}{\sqrt{-k^{3/2}B1}}]))/E1 \qquad (33)$$

The nature and stability of the equilibrium points $\{x_{1,2}, y_{1,2}\}$ vary with the value of the parameter q, and the value of the flow rate q is taken to lie in the interval $(-1,1)$ [10,14]. Qualitative changes, clearly in figure (3), as follows:

- For $-1 < q < -1+\phi$, the equilibrium point is a co-dimensional-two saddle points as depends on ϕ, Ω when $\tau_{1,2} = 0$ and $\zeta_{1,2} < 0$ in this range; see figure 3(a).
- Isolated equilibrium points occur when $q = q_{c1} = -1+\phi$. These are known as non-hyperbolic degenerate points [10,20], since $\tau_{1,2} = 0$ and $\zeta_{1,2} = 0$, these are corresponding to a non-simple degeneracy since $J|_{(\bar{x}_{1,2},\bar{y}_{1,2})} = 0$ and its eigenvalues are zero at this flow [23]; see figure 3(b).
- For $q > -1+\phi$, $\tau_{1,2} = 0$ and $\zeta_{1,2} > 0$, therefore each equilibrium point is stable center as shown in figure 3(c).

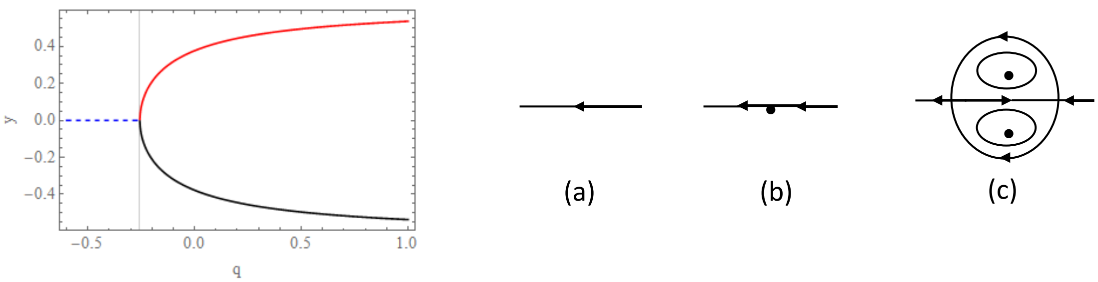

Figure 3: Local bifurcation with(ϕ=0.3,Ω=3.5) diagram for wave crest $x = n\pi$, $n \in Z$ and pictorial topological changes for $(a)\ q < -1+\phi$, $(b)\ q = -1+\phi$, $(c)\ q > -1+\phi$

Depending on the definition of a bifurcation, one occur under wave crest at x=nπ for n ∈Z. This bifurcation is co-dimension three since it depends on the flow rate parameter q, amplitude ratio ϕ and rotation wave Ω, Figure (3) gives a bifurcation diagram in the q-y plane. Various values of the rotation wave and amplitude ratio clearly in figure (4)

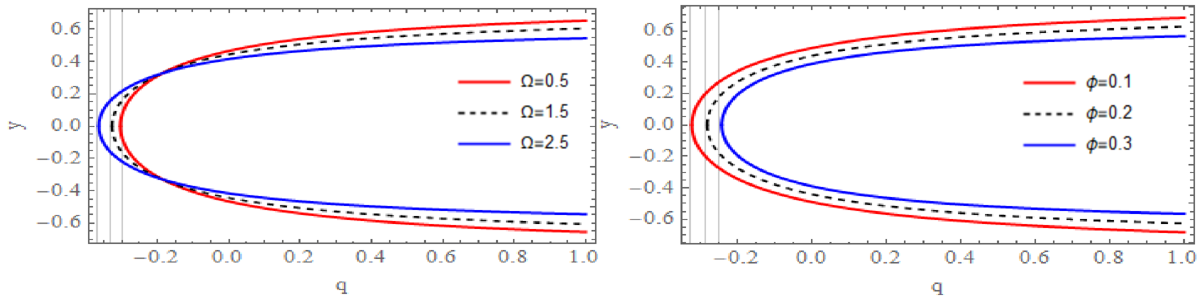

Figure 4: Local bifurcation diagram different values of rotation and amplitude ratio

4.2- the stegnation points $\{x_{3,4}, y_{3,4}\}$

Consider the equilibrium points $\{x_{3,4}, y_{3,4}\} = \{\pm \frac{\sqrt{A+2*B\mathrm{Cos}[B]-\sqrt{k}q\mathrm{Cos}[2*B]+(2*C*D)\mathrm{Sin}[B]+\mathrm{Sin}[2*B]}}{\sqrt{2}\sqrt{\sqrt{k}\phi(E*\mathrm{Cos}[B]+\mathrm{Cos}[2*B]+\sqrt{k}(F+2q\mathrm{Cos}[B])\mathrm{Sin}[B])}}, 0\}$

these critical points lie along the axis for (y=0). The Jacobian at these critical points is

$$J|_{(x_{3,4},y_{3,4})} = \begin{bmatrix} \pm\frac{\partial f}{\partial x} & 0 \\ \pm\frac{\partial g}{\partial x} & 0 \end{bmatrix} \text{ the eigenvalue } \lambda_3 = 0, \text{ and}$$

$$\begin{aligned}\lambda_4 = &-((\sqrt{k}\phi\mathrm{Sin}[\tfrac{\sqrt{2}\sqrt{AA}}{\sqrt{BB}}](CC + 2\sqrt{k}q\mathrm{Cos}[\sqrt{k}(GG + \phi\mathrm{Cos}[\tfrac{\sqrt{2}\sqrt{AA}}{\sqrt{BB}}])] + 4\sqrt{k}\mathrm{Cos}[\sqrt{k}(DD + \phi\mathrm{Sin}[\tfrac{\sqrt{AA}}{\sqrt{2}\sqrt{BB}}]^2)] - \\ &2\sqrt{k}\phi\mathrm{Cos}[\sqrt{k}(DD + \phi\mathrm{Sin}[\tfrac{\sqrt{AA}}{\sqrt{2}\sqrt{BB}}]^2)] + 2\sqrt{k}\phi\mathrm{Cos}[\tfrac{\sqrt{2}\sqrt{AA}}{\sqrt{BB}}](1 - \mathrm{Cos}[\sqrt{k}(DD - \phi + \phi\mathrm{Sin}[\tfrac{\sqrt{AA}}{\sqrt{2}\sqrt{BB}}]^2)] + \sqrt{k}(2 + q - \\ &\phi)\mathrm{Sin}[\tfrac{1}{2}\sqrt{k}(GG + \phi\mathrm{Cos}[\tfrac{\sqrt{2}\sqrt{AA}}{\sqrt{BB}}])])) - 2\mathrm{Sin}[\sqrt{k}(GG + \phi\mathrm{Cos}[\tfrac{\sqrt{2}\sqrt{AA}}{\sqrt{BB}}])] - 4\mathrm{Sin}[\sqrt{k}(DD + \phi\mathrm{Sin}[\tfrac{\sqrt{AA}}{\sqrt{2}\sqrt{BB}}]^2)] + \\ &4k\mathrm{Sin}[\sqrt{k}(DD + \phi\mathrm{Sin}[\tfrac{\sqrt{AA}}{\sqrt{2}\sqrt{BB}}]^2)] + 4kq\mathrm{Sin}[\sqrt{k}(DD + \phi\mathrm{Sin}[\tfrac{\sqrt{AA}}{\sqrt{2}\sqrt{BB}}]^2)] - 4k\phi\mathrm{Sin}[\sqrt{k}(DD + \phi\mathrm{Sin}[\tfrac{\sqrt{AA}}{\sqrt{2}\sqrt{BB}}]^2)] - \\ &2kq\phi\mathrm{Sin}[\sqrt{k}(DD + \phi\mathrm{Sin}[\tfrac{\sqrt{AA}}{\sqrt{2}\sqrt{BB}}]^2)] + k\phi^2\mathrm{Sin}[\sqrt{k}(DD + \phi\mathrm{Sin}[\tfrac{\sqrt{AA}}{\sqrt{2}\sqrt{BB}}]^2)] + k\phi^2\mathrm{Cos}[\tfrac{\sqrt{2}\sqrt{AA}}{\sqrt{BB}}]^2\mathrm{Sin}[\sqrt{k}(DD + \\ &\phi\mathrm{Sin}[\tfrac{\sqrt{AA}}{\sqrt{2}\sqrt{BB}}]^2)]))/\frac{(\sqrt{k}\mathrm{Cos}[\frac{1}{2}\sqrt{k}(GG + \phi\mathrm{Cos}[\frac{\sqrt{2}\sqrt{AA}}{\sqrt{BB}}])](GG + \phi\mathrm{Cos}[\frac{\sqrt{2}\sqrt{AA}}{\sqrt{BB}}])^2 +}{2\mathrm{Sin}[\sqrt{k}(DD + \phi\mathrm{Sin}[\frac{\sqrt{AA}}{\sqrt{2}\sqrt{BB}}]^2)])}\end{aligned} \tag{34}$$

Where AA=A+2 B Cos[B]-$\sqrt{k}$ q Cos[2 B]+2 C D Sin[B]+Sin[2 B];
BB=$\sqrt{k}$ ϕ (E Cos[B]+Cos[2 B]+ $\sqrt{k}$ (F+2 q Cos[B]) Sin[B]); CC=-4 $\sqrt{k}$-2 $\sqrt{k}$ q+2 $\sqrt{k}$ ϕ; DD=1-ϕ; GG=-2+ϕ,

Acoording to above equation, it observed that the Jacobian matrix at the point $\{x_{3,4}, y_{3,4}\}$ has a zero eigenvalue, so this point becomes a non-hyperbolic point. Therefore, the linearization at this point does not reflect the real dynamical behavior around it. Hence we will confine ourselves to investigate the dynamical behavior around this point numerically clear that in figure (5).

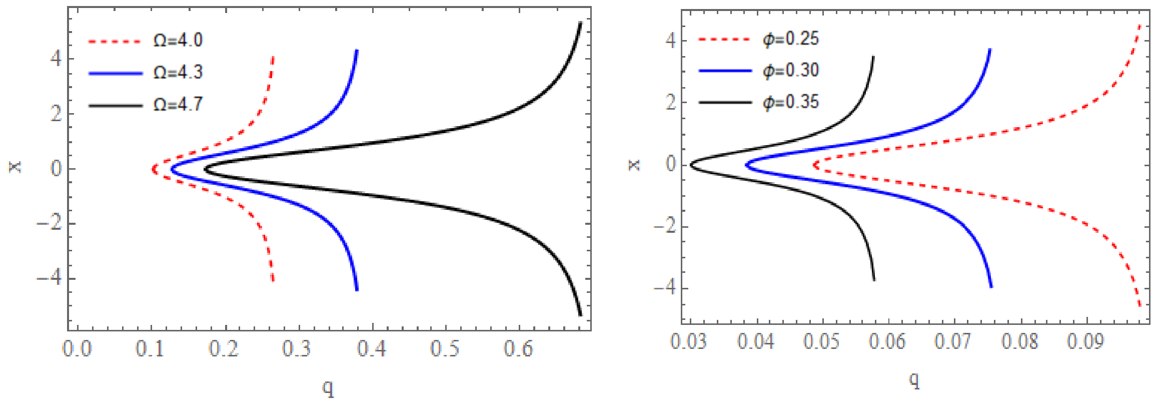

Figure 5: Local bifurcation diagram for $y = 0$

4.3- the stegnation points $\{x_{5,6}, y_{5,6}\}$

The equilibrium points $\{x_{5,6}, y_{5,6}\} = \{\frac{(2n+1)\pi}{2}, \pm \frac{\sqrt{2\sqrt{k}(1+q-q\text{Cos}[\sqrt{k}])-2\text{Sin}[\sqrt{k}]}}{\sqrt{k^{3/2}(1+q)}}\}$, where $n \in Z$, with $q = \frac{\sqrt{k}-\text{Sin}[\sqrt{k}]}{\sqrt{k}(-1+\text{Cos}[\sqrt{k}])}$. The case when q approaches $q_{c2} = \frac{\sqrt{k}-\text{Sin}[\sqrt{k}]}{\sqrt{k}(-1+\text{Cos}[\sqrt{k}])}$ saddle nodes of contiguous waves coalesce below wave troughs, therefore the equilibrium points merge on $x = \frac{(2n-1)\pi}{2}$ for $q = q_{c2}$ to produce a degenerate point containing six heteroclinic connections. For $q > q_{c2}$, the degenerate point bifurcates on the y-branch at $x = \frac{(2n-1)\pi}{2}$ each critical point corresponds to a unstable saddle. The critical points $\{x_{5,6}, y_{5,6}\}$, crop up on vertical below the wave crest. The Jacobian matrix is

$J|_{\{x_{5,6},y_{5,6}\}} = \begin{bmatrix} 0 & S_1 \\ S_2 & 0 \end{bmatrix}$, and the eigenvalues:

$$S_1 = \frac{k(1+q)\text{Sin}\left[\frac{\sqrt{k}\sqrt{2\sqrt{k}(1+q-q\text{Cos}[\sqrt{k}])-2\text{Sin}[\sqrt{k}]}}{\sqrt{k^{3/2}(1+q)}}\right]}{\sqrt{k}\text{Cos}[\sqrt{k}]-\text{Sin}[\sqrt{k}]},$$

$$S_2 = \frac{k(2+q)\phi - kq\phi\text{Cos}[2\sqrt{k}] + \sqrt{k}\phi\left(-2\text{Cos}\left[\frac{\sqrt{2\sqrt{k}(1+q-q\text{Cos}[\sqrt{k}])-2\text{Sin}[\sqrt{k}]}}{k^{1/4}\sqrt{1+q}}\right](\sqrt{k}\text{Cos}[\sqrt{k}]+(-1+k+kq)\text{Sin}[\sqrt{k}]) - \text{Sin}[2\sqrt{k}]\right)}{(-\sqrt{k}\text{Cos}[\sqrt{k}]+\text{Sin}[\sqrt{k}])^2}.$$

$$\lambda_{5,6}=\pm\frac{1}{(-\sqrt{k}\mathrm{Cos}[\sqrt{k}]+\mathrm{Sin}[\sqrt{k}])^2}\sqrt{k}\sqrt{(}-\sqrt{k}(1+q)\phi(\sqrt{k}\mathrm{Cos}[\sqrt{k}]-\mathrm{Sin}[\sqrt{k}])(-\sqrt{k}(2+q)+\sqrt{k}q\mathrm{Cos}[2\sqrt{k}]+$$
$$2\mathrm{Cos}[\frac{\sqrt{2\sqrt{k}(1+q-q\mathrm{Cos}[\sqrt{k}])-2\mathrm{Sin}[\sqrt{k}]}}{k^{1/4}\sqrt{1+q}}](\sqrt{k}\mathrm{Cos}[\sqrt{k}]+(-1+k+kq)\mathrm{Sin}[\sqrt{k}])+$$
$$\mathrm{Sin}[2\sqrt{k}])\mathrm{Sin}[\frac{\sqrt{k}\sqrt{2\sqrt{k}(1+q-q\mathrm{Cos}[\sqrt{k}])-2\mathrm{Sin}[\sqrt{k}]}}{\sqrt{k^{3/2}(1+q)}}]) \tag{35}$$

Qualitative changes of critical points for $q=\frac{\sqrt{k}-\mathrm{Sin}[\sqrt{k}]}{\sqrt{k}(-1+\mathrm{Cos}[\sqrt{k}])}$ and $x=\frac{(2n-1)\pi}{2}$ occurs follows:

- For $q=q_{c2}$, $\tau_{56}=0$ and $\xi_{5,6}$=0, the critical pointid degenerate with non-simple degeneracy since $J|_{\{x_{5,6},y_{5,6}\}}=\det matrix$=0, see figure 6(b).
- For $q>\frac{\sqrt{k}-\mathrm{Sin}[\sqrt{k}]}{\sqrt{k}(-1+\mathrm{Cos}[\sqrt{k}])}$, $\tau_{56}=0$ and $\xi_{5,6}<0$, the critical points are saddle, see figure 6(c). A bifurcation diagram for (q-y) plane and pictorial taplovical change sre showing in figure(6).

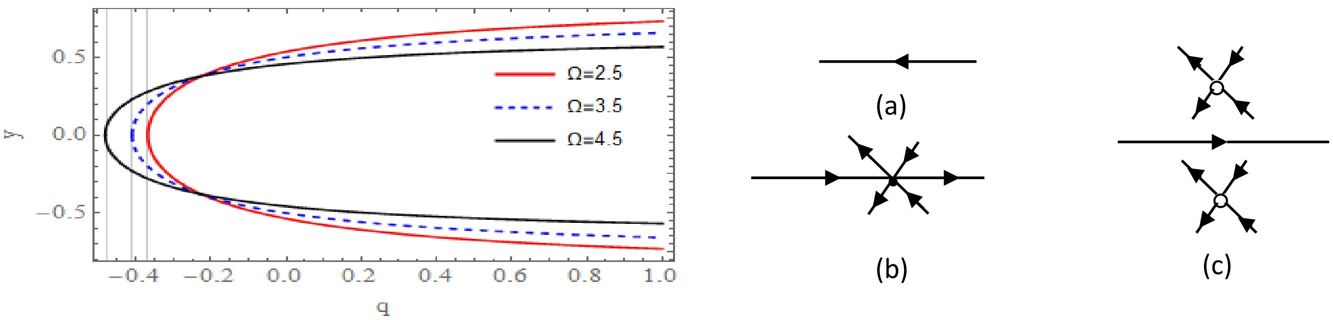

Figure 6: Local bifurcation diagram for wave below crest $x=\frac{(2n-1)\pi}{2}$, $n\in Z$ and pictorial topological changes for $(a)\ q<\frac{\sqrt{k}-\mathrm{Sin}[\sqrt{k}]}{\sqrt{k}(-1+\mathrm{Cos}[\sqrt{k}])}$, $(b)\ q=\frac{\sqrt{k}-\mathrm{Sin}[\sqrt{k}]}{\sqrt{k}(-1+\mathrm{Cos}[\sqrt{k}])}$, $(c)\ q>\frac{\sqrt{k}-\mathrm{Sin}[\sqrt{k}]}{\sqrt{k}(-1+\mathrm{Cos}[\sqrt{k}])}$

For y=0, the associative vector field reduce to $\{\dot{x},\dot{y}\}=\{\frac{-\sqrt{k}(h+q-q\mathrm{Cos}[h\sqrt{k}])+\mathrm{Sin}[h\sqrt{k}]}{h\sqrt{k}\mathrm{Cos}[h\sqrt{k}]-\mathrm{Sin}[h\sqrt{k}]},0\}$, from which

$\xi=\frac{-\sqrt{k}(h(x)+q-q\mathrm{Cos}[h(x)\sqrt{k}])+\mathrm{Sin}[h(x)\sqrt{k}]}{h(x)\sqrt{k}\mathrm{Cos}[h(x)\sqrt{k}]-\mathrm{Sin}[h(x)\sqrt{k}]}$; critical conditions appear at $\bar{x}=n\pi$ and wave $\bar{x}=(2n-1)\pi/2$. Bifurcation curves are follows:

$f(\bar{x},\bar{y},\beta)=\xi(\bar{x},\beta)=0$, then

$$\xi|_{\bar{x}=n\pi}=\frac{\sqrt{k}(1+q-\phi-q\mathrm{Cos}[\sqrt{k}(-1+\phi)])+\mathrm{Sin}[\sqrt{k}(-1+\phi)]}{\sqrt{k}(-1+\phi)\mathrm{Cos}[\sqrt{k}(-1+\phi)]+\mathrm{Sin}[\sqrt{k}(1-\phi)]}=0, \tag{36}$$

$$\xi|_{\bar{x}=(2n-1)\pi/2}=\frac{\sqrt{k}(-1-q+q\mathrm{Cos}[\sqrt{k}])+\mathrm{Sin}[\sqrt{k}]}{\sqrt{k}\mathrm{Cos}[\sqrt{k}]-\mathrm{Sin}[\sqrt{k}]}=0. \tag{37}$$

The global bifurcation diagram has the following curves:

$$W = \{(\emptyset, \mathrm{q}): 0 < \emptyset < 1, \mathrm{q} = (\sqrt{k} - \sqrt{k}\,\phi + \mathrm{Sin}[\sqrt{k}\,(-1+\phi)])/(\sqrt{k}\,(-1 + \mathrm{Cos}[\sqrt{k}\,(-1 + \phi)]))\}, \quad (38)$$

$$Z = \{(\emptyset, \mathrm{q}): 0 < \emptyset < 1, \mathrm{q} = \frac{\sqrt{k} - \mathrm{Sin}[\sqrt{k}]}{\sqrt{k}(-1 + \mathrm{Cos}[\sqrt{k}])}. \quad (39)$$

Along the bifurcation curve W, a non-simple degenerate point exist under the wave crests, which is an isolated non-hyperbolic degenerate point. Whereas along the bifurcation curve Z, adjacent equilibrium points join together below the wave troughs and form connections of non-simple degenerate points. Equilibrium points that combine on Z to produce a degenerate saddle have six heteroclinic paths. Figure (7) is traced to show the bifurcation curves. The region of flow is classified as follows:

- When all flow fluid to opposite direction of the wave motion then is called backward flow.
- the trapping is occur when the critical points, which is saddle, linked by heteroclinic connections and the interaction of two vortices opposite rotation exist.
- The flow is called augmented, when the eddies below of the crests wave combine and compose heteroclinic connection with the neighbors and the transport some fluid through the centerline in the wave direction.

5- Results and Discussions

when we applied our problem to a Bingham fluid and plotted various types of streamline topology and their bifurcation clearly in figures (3-9). The stability and nature of equilibrium points $\{x_{1,2}, y_{1,2}\}$ and their bifurcations shown in figure (3). It is shown that, at $q = q_{c1}$, an unstable equilibrium points bifurcates into two stable centers below wave crest. Figure (4) shown the bifurcation of different values of the rotation and amplitude ratio. Clear that in figure (5) the point becomes a non-hyperbolic point the linearization at this point does not reflect the real dynamical behavior around it. Hence we will confine ourselves to investigate the dynamical behavior around this point numerically. When flow rate q approaches to, the unstable equilibrium points on the longitudinal axis join together and form a non-simple degenerate point with six heteroclinic connections as given in figure (6). When fixed the values of (ϕ, Ω) and given different values of q we notes the stability of equilibrium points along with the transitions of streamline patterns for Bingham fluid the streamline patterns for degenerate are given in panels (B, D). two possible bifurcations appear as q, Ω and ϕ are varied. Panels (A-C) give the transform of stability of equilibrium points and formation of vortex region below wave crest. The uniting of these neighboring vortex regions are indicated in figure 7 (C-E). The unstable saddle nodes on the longitudinal axis coincide under wave trough and lift up to produce heteroclinic connections between saddles. In figure (8) the eddying increasing when the value of Ω is increasing and centuries around the point with fixed values of (q, ϕ). The value of ϕ active to moves of eddying and number of this eddying clearly in figure (9).

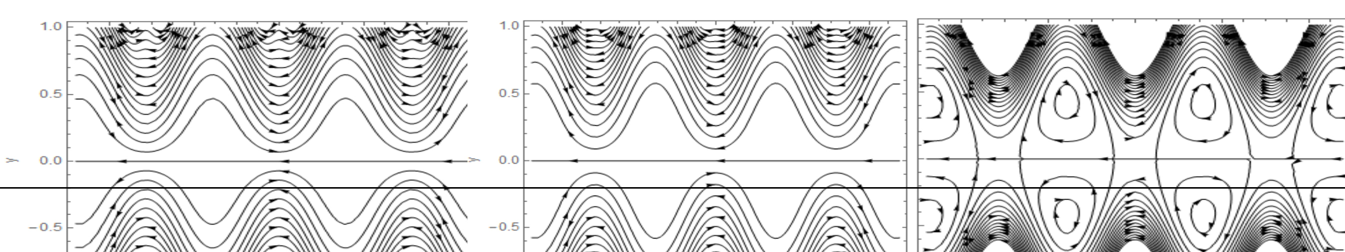

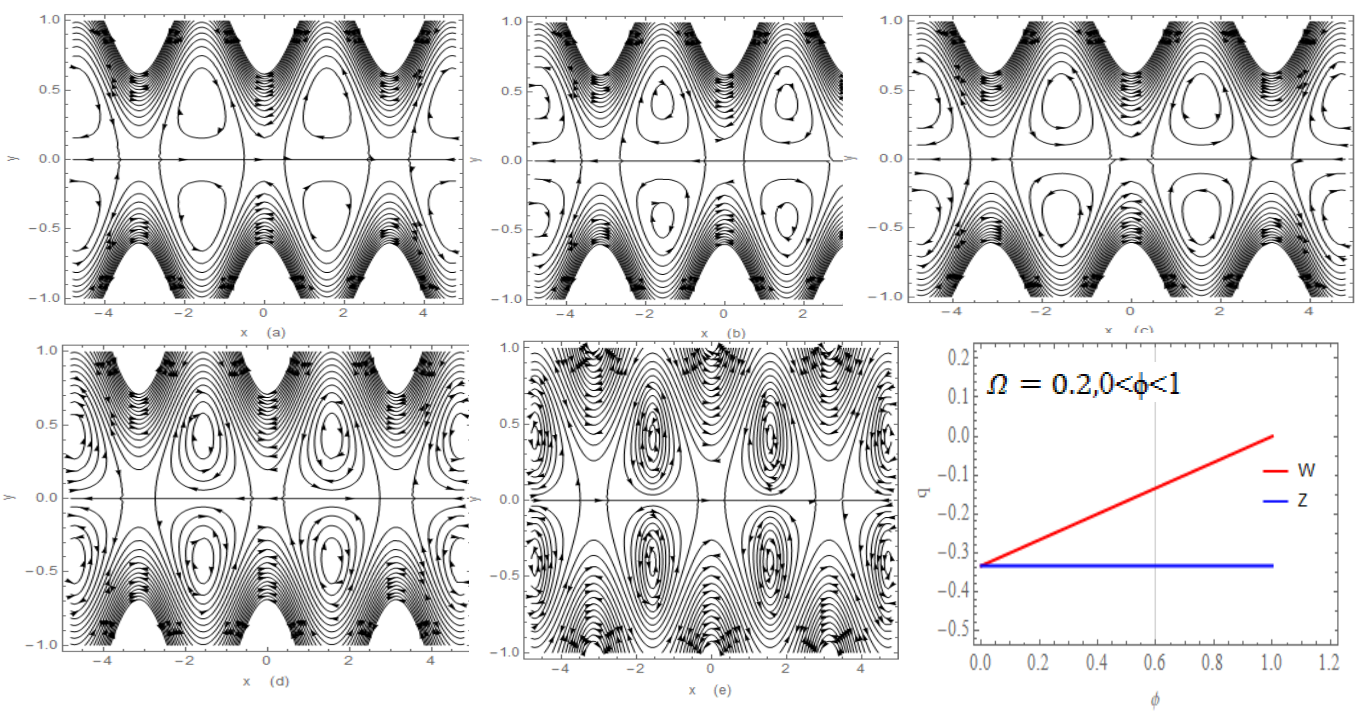

Figure 8: Global bifurcation diagram for planer flow. (a-e) corresponding to ($\phi = 0.6$ and q= -0.18) with different value of Ω:. (a)=0.2, (b)= 2.0, (c)= 3.0, (d)= 5.0 and (e)= 6.0

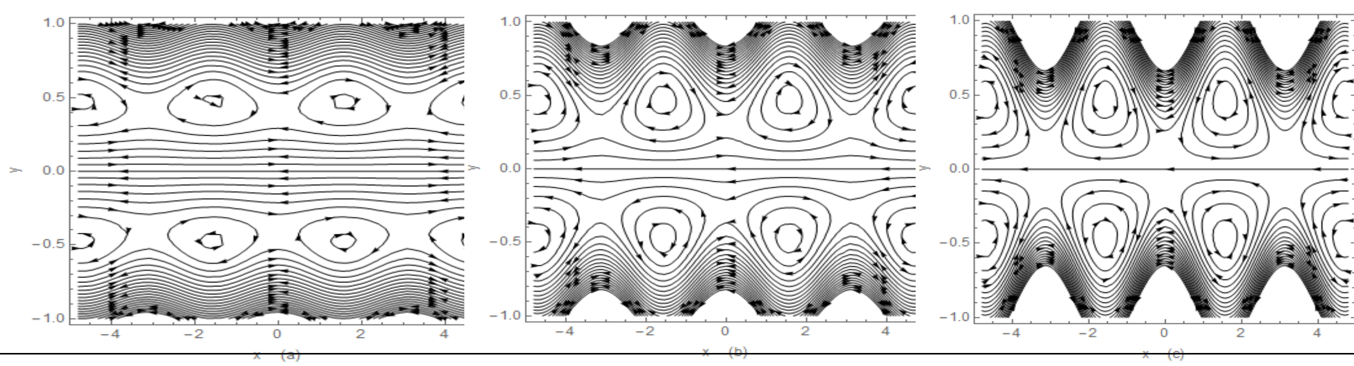

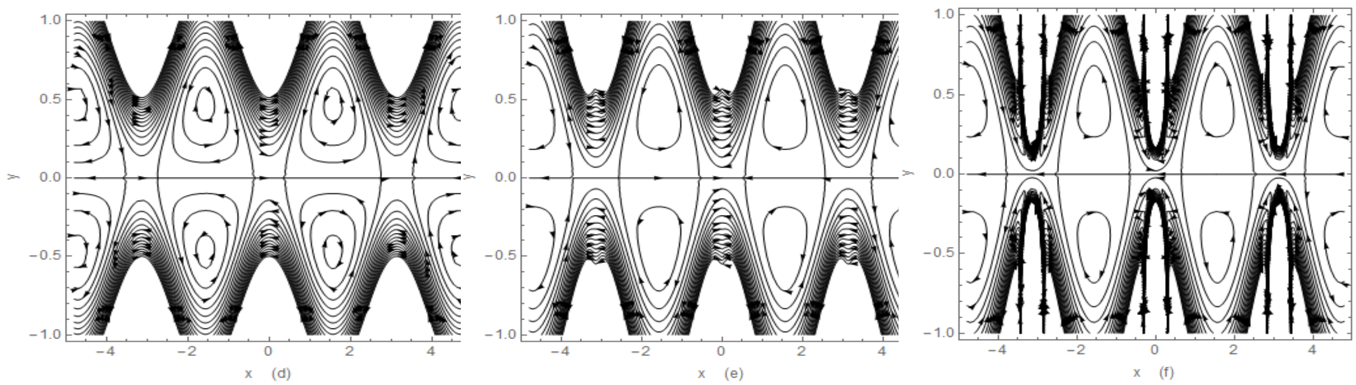

Figure 9: Global bifurcation diagram for planer flow. (a-f) corresponding to ($\Omega = 2.0$ and q= -0.18) with different value of ϕ:. (a)=0.1, (b)= 0.3, (c)= 0.5, (d)= 0.7, (e) = 0.85 and (f)= 0.95

6- Conclusion

In this reseach, we studied the effect of the rotation on the streamline patterns and their bifurcaions in 2-dimension peristaltic flow of non-Mewtonian fluid in symmetric channel therefore the possible nature of critical points were either saddle or center. using by inspection of eigenvalues of the Jacobian matrix, it was classification of the critical points. The apply this principle till to the detected the local bifurcation of the critical points obverse for different flow case. Three different flow cases manifest themselve: backward, trapping and augmented flow. The key findings of the performed analysis are:

a- Saddle, saddle or center nodes are found on the center line, down of the wave peaks and wave throughs the channel walls.

b- Three different flow cases manifest themselve: backward, trapping and augmented flows are found.

c- Observed that the Jacobian matrix at the point $\{x_{3,4},\ y_{3,4}\}$ has a zero eigenvalue, so this point becomes a non-hyperbolic point. Therefore, the linearization at this point does not reflect the real dynamical behavior around it.

d- The increasing in the q up to an best value causes the backward region to retract and after that an opposite demeanor is recorded.

e- The increasing of the rotation value implies that increasing of number of blouse and reduce trapping and it near to the centerline.

f- When arrived amplitude ratio to best value implies that number of blouse are increasing and near to centerline otherwise it is near the channel walles.

References

[1] T.W. Latham ,M.S. Thesis , MIT, Cambridge (1966).

[2] Jaffrin, M.Y., Shapiro, A.H. and Weinberg, S.L. “peristaltic pumping with long wavelength at low Reynolds numbers,” *Journal of Fluid Mechanic*, 37: 799-825, 1969.

[3] A. M. Abd-All, S.M. Abo-Dahab, H.D. El-Shahrany, “Effect of rotation and initial stress on peristaltic transport of fourth grade fluid with heat transfer and induced magnetic field,” Journal of Magnetism and Magnetic Materials, 349: 268-280, 2014.

[4]] A.M. Abd-Alla, S.M. Abo-Dahab, “Rotation effect on peristaltic transport of a Jeffrey fluid in an asymmetric channel with gravity field,” *Alexandria Engineering Journal* Vol. 55, 2016.

[5] B. REDDAPPA1, A. PARANDHAMA, S. SREENADH, ” PERISTALTIC TRANSPORT OF CONDUCTING WILLIAMSON FLUID IN A POROUS CHANNEL ” *J. Math. Comput. Sci.* 10 (2020), No. 2, 277-288,https://doi.org/10.28919/jmcs/4367.

[6] Marco Marconati , Sharvari Raut , Farshad Charkhi , Adam Burbidge, Jan Engmann, and Marco Ramaioli, “Transient peristaltic transport of grains in a liquid”, *EPJ Web of Conferences 140*, 09009 (2017), DOI: 10.1051/epjconf/201714009009.

[7] H. Tariq and A. A. Khan, “Peristaltic transport of a second-grade dusty fluid in a tube”, *Journal of Mechanical Engineering Research,* Vol. 11(2), pp. 11-25, DOI 10.5897/JMER2019.0518,(2020).

[8] M. A. Murad, A. M. Abdulhad, “Peristaltic Transport of Power-Law Fluid in an Elastic Tapered Tube with Variable Cross-Section Induced by Dilating Peristaltic Wave”, *Iraqi Journal of Science*, Vol 62 No 4, DOI: https://doi.org/10.24996/ijs.2021.62.4.25 ,(2021).

[9] C. Rajashekhar, G. Manjunatha, K. V. Prasad, B. B. Divya & Hanumesh Vaidya, “Peristaltic transport of two-layered blood flow using Herschel–Bulkley Model”, *Cogent Engineering* 5: 1495592, DOI: 10.1080/23311916.2018.1495592, (2018).

[10] Joel Jiménez-Lozano and Mihir Sen, “Streamline topologies of two-dimensional peristaltic flow and their bifurcations”, *Chemical Engineering and Processing*, 49, 704-715, (2010).

[11] Z. Asghar and N. Ali, “Slip effects on streamline topologies and their bifurcations for peristaltic flows of a viscous fluid”, *Chin. Phys.* B, 23(6)- 064701,(2014).

[12] Z. Asghar and N. Ali, “Streamline topologies and their bifurcations for mixed convective peristaltic flow”, *AIP Advances* **5**, 097142, doi: 10.1063/1.4931088, (2015).

[13] Ali, N. and Ullah, “ Bifurcation Analysis for Peristaltic Transport of a Power-Law Fluid”, *Z. Naturforsch. A* 74(3), 213–225, (2019).

[14] Ullah, K., Ali,N. and Sajid, M, “Bifurcation and stability analysis of critical/stagnation points for peristaltic transport of a power-law fluid in a tube”, *Journal of the Brazilian Society of Mechanical Sciences and Engineering,* 41(10), 420, (2019).

[15] Ali, N., Ullah, K. and Rasool, H., "Bifurcation analysis for a two-dimensional peristaltic driven flow of power-law fluid in asymmetric channel", *Phys. Fluids* 32, 073104 (2020), doi: 10.1063/5.0011465, (2020).

[16] Ullah, K. and Ali,N., " A study on bifurcation of stagnation points for a peristaltic transport of micropolar fluids with slip condition", *Physica Scripta, 96,025207,* doi.org: 10.1088/1402-4896/abccel, (2021).

[17] M. A. Murad, (2021) " Flow Analysis of non-Newtonian, Herschel-Bulkley Fluids and Some of Its Special cases", Thesis, Phd, university of Baghdad, College of Science.

[18] Hayat, T., Noreen, S., Shabab Alhothuali, M., Asghar, S. and Alhomaidan. A., " Peristaltic flow under the effect of an induced magnetic field and heat and mass transfer*", International Journal of Heat and Mass Transfer,* 55, 443-452, (2012).

[19] Y. Wang, *Acta Mechanica* 186, 187 (2006).

[20] L.Perko, (2000), " differential Equation and Dynamical System", Springer.

[21] P. G. Bakker, (1991), "Bifurcation in Flow Patterns", Kluwer Academic Publishers.

[22] Seydel, R., (1988), From Equilibrium to Chaos: Practical Bifurcation and Stability Analysis, Elsevier.

[23] Gürcan, F. and Deliceoglu, A. , "Streamline topologies near nonsimple degenerate points in two dimensional flows with double symmetry away from boundaries and an application", *Physics of Fluids*, 17, 093106–0931067-0931067, (2005).